Structure
Article

Separation-of-Function Mutants Unravel the Dual-Reaction Mode of Human 8-Oxoguanine DNA Glycosylase

Bjørn Dalhus,[1,2,*] Monika Forsbring,[1] Ina Høydal Helle,[1,2] Erik Sebastian Vik,[1] Rune Johansen Forstrøm,[1] Paul Hoff Backe,[1,2] Ingrun Alseth,[1] and Magnar Bjørås[1,2]
[1]Centre for Molecular Biology and Neuroscience (CMBN) and Institute of Medical Microbiology, Rikshospitalet, Oslo University Hospital, N-0027 Oslo, Norway
[2]Institute of Clinical Biochemistry, University of Oslo, N-0027 Oslo, Norway
*Correspondence: bjorn.dalhus@rr-research.no
DOI 10.1016/j.str.2010.09.023

SUMMARY

7,8-Dihydro-8-oxoguanine (8oxoG) is a major mutagenic base lesion formed when reactive oxygen species react with guanine in DNA. The human 8oxoG DNA glycosylase (hOgg1) recognizes and initiates repair of 8oxoG. hOgg1 is acknowledged as a bifunctional DNA glycosylase catalyzing removal of the damaged base followed by cleavage of the backbone of the intermediate abasic DNA (AP lyase/β-elimination). When acting on 8oxoG-containing DNA, these two steps in the hOgg1 catalysis are considered coupled, with Lys249 implicated as a key residue. However, several lines of evidence point to a concurrent and independent monofunctional hydrolysis of the *N*-glycosylic bond being the in vivo relevant reaction mode of hOgg1. Here, we present biochemical and structural evidence for the monofunctional mode of hOgg1 by design of separation-of-function mutants. Asp268 is identified as the catalytic residue, while Lys249 appears critical for the specific recognition and final alignment of 8oxoG during the hydrolysis reaction.

INTRODUCTION

Reactive oxygen species arise endogenously as by-products of aerobic respiration (Ames et al., 1993) and after exposure to external sources like ionizing radiation (Zhang et al., 1997), H_2O_2, or carcinogens (Lindahl and Wood, 1999). Several types of oxidative DNA base lesions are formed, including 7,8-dihydro-8-oxoguanine (8oxoG) (Figure 1A), a major oxidized purine lesion with a highly mutagenic potential (Kasai et al., 1986). Oxidized bases are mainly repaired by the base excision repair (BER) pathway (Figure 1B), initiated by specific DNA glycosylases that recognize and remove the modified bases by hydrolysis of the *N*-glycosylic bond between the deoxyribose and the damaged base (Dalhus et al., 2009; Hegde et al., 2008; Krokan et al., 1997; Seeberg et al., 1995; Wood et al., 2001). The major human DNA glycosylase for removal of 8oxoG, hOgg1, was cloned based on sequence homology with the *Saccharomyces cerevisiae* 8oxoG DNA glycosylase Ogg1 (Aburatani et al., 1997; Bjørås et al., 1997; Lu et al., 1997; Radicella et al., 1997; Roldan-Arjona et al., 1997; Rosenquist et al., 1997).

DNA glycosylases are classified as mono- or bifunctional based on the nature of the base removal and the enzymes' ability to cleave abasic DNA. Monofunctional DNA glycosylases catalyze only the hydrolysis of the *N*-glycosylic bond (Figures 1B and 1C). A highly conserved basic residue is believed to charge-stabilize an oxocarbenium intermediate formed during cleavage of the *N*-glycosylic bond (McCann and Berti, 2008; Werner and Stivers, 2000). Interestingly, some DNA glycosylases, like human Tdg (Maiti et al., 2008), vertebrate Smug1 (Wibley et al., 2003), and prokaryotic Mug (Barrett et al., 1998) do not possess carboxylate residues in the active site, and, consistent with this, have several orders of magnitude lower excision rates. The product of the base hydrolysis is an apurinic/apyrimidinic site (abasic/AP site), which in turn is processed by an AP endonuclease that incises the sugar phosphate backbone 5′ of the lesion to form a 5′-dRP residue (Figure 1C). This remnant of the damaged base is removed by the 5′-dRPase activity of DNA polymerase β (Polβ), which also incorporates a new nucleotide to restore the DNA (Figure 1B). This monofunctional mode is common to both the human alkylbase DNA glycosylase Aag (Lau et al., 2000), the uracil DNA glycosylase UDG (Mol et al., 1995), the canonical helix-hairpin-helix (HhH) 3-methyl adenine DNA glycosylase AlkA (Labahn et al., 1996), and the newly described HEAT-repeat like DNA glycosylase AlkD (Dalhus et al., 2007), all prototypical representatives of different structural classes of DNA glycosylases (Dalhus et al., 2009).

In contrast, bifunctional DNA glycosylases/AP lyases both remove the damaged base and cleave the sugar-phosphate backbone at AP sites via a covalent Schiff base intermediate connecting the C1' carbon of the DNA ribose to a primary or secondary amino group in the enzyme (Bailly et al., 1989; Dodson et al., 1994; Kow and Wallace, 1987). The DNA is released by a conjugate elimination mechanism creating a nick in the DNA backbone 3′ of the damaged base (Figure 1D). The AP lyase activity of the bifunctional glycosylases can also act directly on intact AP sites in DNA. Lys249 in hOgg1 has been identified as the residue forming the Schiff base by trapping of the enzyme-DNA complex (Nash et al., 1997). Mutation of the

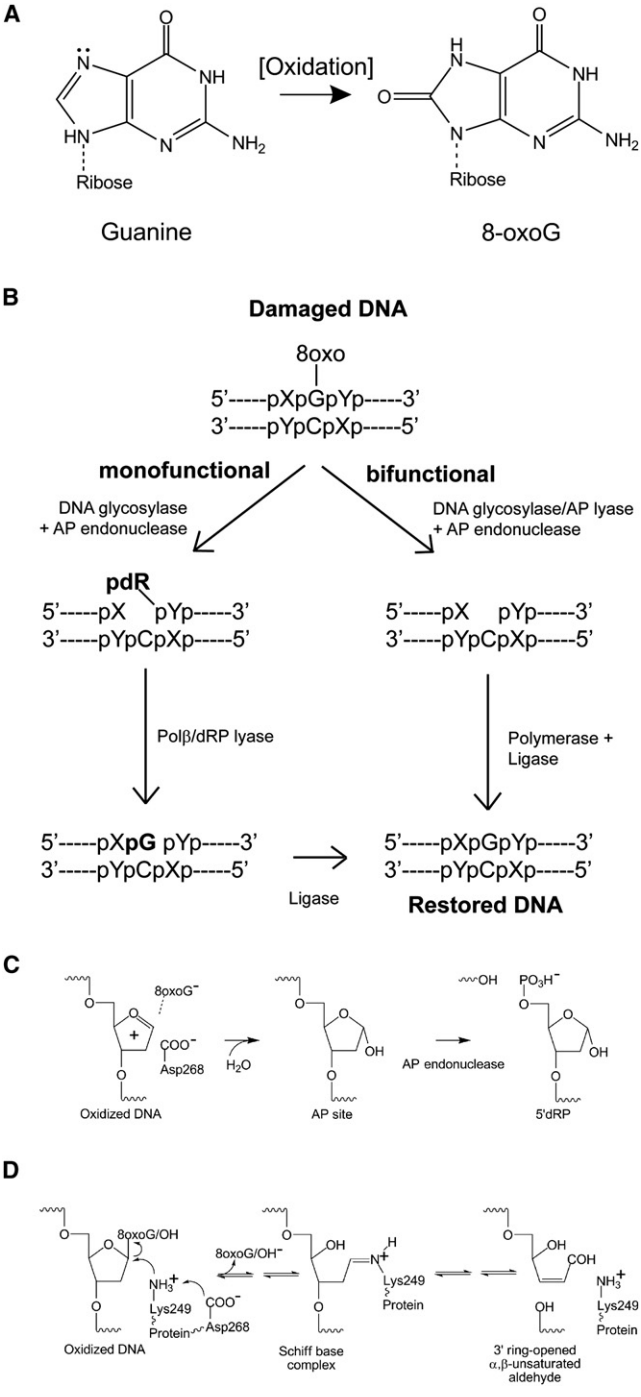

Figure 1. Reaction Mechanisms of Mono- and Bifunctional DNA Glycosylases

(A) Scheme showing molecular structure of guanine and the oxidation product 8oxoG.

(B) Scheme showing subpathways of the base excision repair (BER) pathway for monofunctional DNA glycosylases versus bifunctional DNA glycosylases/AP lyases.

(C) Putative monofunctional mechanism of hOgg1, assuming the reaction proceeds through an oxocarbenium ion (McCann and Berti, 2008; Werner and Stivers, 2000) charge-stabilized by the conserved Asp268 and subsequently reacting with a water nucleophile to form an AP site. The AP site containing DNA is incised by an AP endonuclease. The broken line shows the lysis of the *N*-glycosylic bond.

(D) Simplified description of the acknowledged bifunctional (8oxoG) and AP lyase (OH) mechanisms of hOgg1, with Lys249 forming a covalent Schiff base intermediate (Bruner et al., 2000; Dodson et al., 1994; Nash et al., 1997; Norman et al., 2001) and with Asp268 playing a role in activation of the Lys249 nucleophile. The intermediate Schiff base protein-DNA complex is resolved by hydrolysis with water resulting in β-elimination and 3′ strand insicion.

invariant Asp268 has a dramatic effect on the catalytic activity of hOgg1 (Bjørås et al., 2002; Norman et al., 2003). Accordingly, it has been suggested that Asp268 could be part of the AP lyase reaction by abstracting a proton from Lys249 in the very first step of the β-elimination reaction (Bjørås et al., 2002; Bruner et al., 2000) (Figure 1D). Another role for Asp268 could be in electrostatic stabilization of the developing positive charge of the oxocarbenium ion in base hydrolysis (Norman et al., 2001, 2003). The resulting nicked DNA is further processed by the major human AP endonuclease Ape1 to remove the remains of the nucleotide by 5′ incision, forming a single-nucleotide gap (Figure 1B). This dual mode has been observed for a series of DNA glycosylases involved in repair of oxidative damages in particular, including the *Escherichia coli* DNA glycosylase families endonuclease III (Nth, Asahara et al., 1989), endonuclease VIII (Nei, Melamede et al., 1994) and formamidopyrimidine DNA glycosylase (MutM/Fpg, Boiteux et al., 1990) as well as the eukaryotic analogs Nth1 (Aspinwall et al., 1997), endonuclease VIII-like DNA glycosylases Neil1 (Hazra et al., 2002a) and Neil2 (Hazra et al., 2002b), and the present Ogg1. The identities of the amino groups involved in the Schiff base reaction have been established by trapping of the enzyme-DNA complexes by reduction with $NaBH_4$ (Fromme and Verdine, 2003; Lavrukhin and Lloyd, 2000; Nash et al., 1997; Zharkov et al., 2002).

However, several recent experiments by our laboratory and others suggest that the in vivo relevant mechanism of hOgg1 is a monofunctional mode with removal of the 8oxoG nucleobase only (Allinson et al., 2001; Hill et al., 2001; Kuznetsov et al., 2005; Morland et al., 2005; Vidal et al., 2001; Zharkov et al., 2000b). Particularly, the AP lyase cleavage of abasic DNA by hOgg1 is inhibited in presence of free 8oxoG, and Schiff base formation is abrogated under physiological concentrations of magnesium ions, which also modulate the DNA glycosylase/AP lyase ratio (Morland et al., 2005). Further, abasic DNA is cleaved at a much lower rate than base hydrolysis of the *N*-glycosylic bond (Hill et al., 2001; Norman et al., 2003), and the major human AP endonuclease Ape1 stimulates hOgg1 to bypass the AP lyase step (Hill et al., 2001; Vidal et al., 2001), leaving abasic sites as the major product. Nonconcurrent base release and strand cleavage have been observed for the related murine variant of Ogg1. Indeed, analysis of mouse Ogg1 shows that the hydrolysis of 8oxoG is much faster than the AP lyase reaction (Zharkov et al., 2000b). For the human Ogg1, the base hydrolysis reaction has a reaction rate approximately ten times higher than that of the AP lyase reaction (Kuznetsov et al., 2005). All together these observations support the notion that the DNA glycosylase and AP lyase activities of hOgg1 are uncoupled, and that the AP lyase reaction is much slower than base hydrolysis. Analysis of 8oxoG repair in mammalian cell extracts have demonstrated that BER of

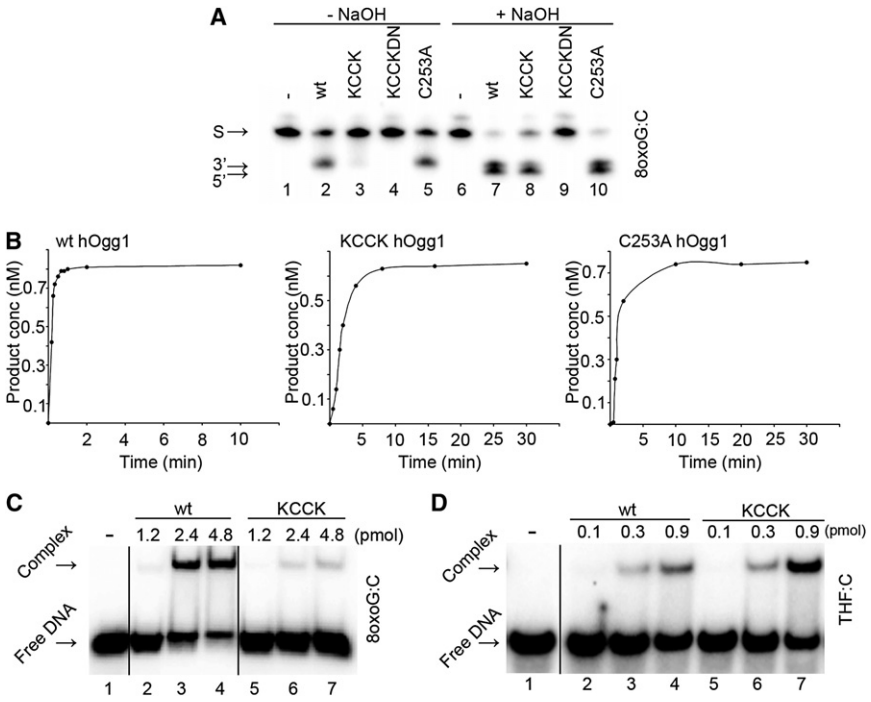

Figure 2. Enzymatic Activities and 8oxoG and Abasic DNA Binding of hOgg1 Separation-of-Function Mutants

(A) 8oxoG DNA glycosylase assay of WT and mutant hOgg1. 0.75 pmol protein was mixed with 10 fmol substrate DNA and incubated at 37°C for 30 min. Half of the reaction was treated with NaOH (+) to generate strand breaks at abasic sites.

(B) Single-turnover kinetics experiment of WT, KCCK and C253A mutants of hOgg1 on 8oxoG DNA. Curves show representative series. Using the mean values of three independent experiments, a fit to a one phase associate model was used for the calculation of the catalytic turnover rate k_{obs} (min^{-1}).

(C and D) EMSA of WT and KCCK mutant hOgg1 binding to 8oxoG-containing and abasic DNA. Duplex DNA (10 fmol) containing either 8oxoG:C (C) or AP site analog THF:C (D) was incubated (15 min on ice) with 50-fold excess of nondamaged DNA (competitor), hOgg1 as stated, or no enzyme (-). Three parallel experiments were performed and representative gels are shown in the respective panels.

See also Figure S1 for further EMSA of mutants KCCKDN and C253A with 8oxoG and all protein variants with undamaged DNA.

these lesions depend upon the 5′-terminal deoxyribose phosphatase (5′-dRPase) activity of DNA polymerase β (Allinson et al., 2001), further suggesting that an intact abasic site, subsequently processed by Ape1 to yield a 5′-dRP terminus, is the major product of hOgg1 in vivo.

In order to identify the molecular basis of this putative independent monofunctional mode of hOgg1, to identify the residues involved in hydrolysis of the *N*-glycosylic bond as well as to resolve the conundrum of the primary roles of Lys249 and Asp268, in particular, we have designed hOgg1 mutants deficient in AP lyase activity, yet capable of recognizing and processing DNA with 8oxoG. In addition to its role as a nucleophile in the AP lyase reaction (Nash et al., 1997), it has been proposed that Lys249 is important for specific recognition of 8oxoG versus normal guanine partly through formation of an electrostatic dipole between the $Lys249^{+}$ and $Cys253^{-}$ side chains (Banerjee et al., 2005). The observations that several Lys249 mutants are inactive (Nash et al., 1997) additionally suggest that Lys249 plays a critical role in lesion recognition during base hydrolysis. With these observations in mind, we reasoned that an "inverted-dipole" double mutant K249C/C253K (KCCK) could have the properties we sought—a Lys side chain in the active site participating in lesion recognition, but too distant from the C1' atom to form the Schiff base intermediate in the AP lyase reaction.

Biochemical and structural analysis of our designed separation-of-function mutants of hOgg1 presented here reveal Asp268 as the catalytic residue responsible for the monofunctional mode, accounting for the majority of the 8oxoG removal. Our data further suggest that Lys249 is critical for selective recognition and final alignment of the 8oxoG lesion during base hydrolysis, and we propose that the weak AP lyase activity of hOgg1 is a consequence of the proximity of the critical terminal ε-amino group of Lys249 and the C1' ribose atom rather than an essential function of hOgg1.

RESULTS AND DISCUSSION

hOgg1 Has an Autonomous Monofunctional Activity

Purified wild-type (WT) and KCCK-hOgg1 proteins were incubated with 8oxoG-containing double-stranded DNA. The product mixtures were divided in two, and one aliquot was treated with NaOH to cleave intact AP sites before fragment analysis on a denaturing PAGE gel. The KCCK mutant showed no detectable AP lyase activity compared to WT hOgg1 (Figure 2A, lanes 2 and 3) but significant removal of the 8oxoG base (Figure 2A, lanes 7 and 8). This monofunctional activity of the separation-of-function KCCK mutant demonstrates that Ogg1 indeed contains a residue capable of catalyzing the excision of 8oxoG by an independent base hydrolysis mechanism.

Since steady-state kinetic analysis of these mutants do not reveal much information on the most interesting steps of the reaction, as product release is rate-limiting, we performed single-turnover experiments to compare the kinetics of 8oxoG removal by WT and the KCCK mutant protein (Table 1 and Figure 2B). The KCCK mutant showed a k_{obs} value of one-tenth of that of WT enzyme (Table 1). Previous analysis of murine Ogg1 shows that the hydrolysis of 8oxoG is much faster than the AP lyase reaction (Zharkov et al., 2000b) and for human Ogg1, the base hydrolysis reaction is about ten times higher than that of the AP lyase reaction (Kuznetsov et al., 2005). In the present study, we find a 25-fold difference (Table 1). Thus, our data on the KCCK separation-of-function mutant support several other studies suggesting that hOgg1 mainly operates as a monofunctional DNA glycosylase in vivo. Particularly, the AP lyase

Table 1. Kinetic Parameters of WT, KCCK and C253A hOgg1 Glycosylase Activity for Removal of 8oxoG, and WT and C253W hOgg1 AP Lyase Activity

Protein	k_{obs} (min^{-1})
8oxoG hydrolysis	
WT	5.2 ± 0.5
KCCK[a]	0.46 ± 0.09
C253A	0.45 ± 0.03
AP lyase	
WT	0.21 ± 0.07
C253W	0.045 ± 0.017

The catalytic turnover rates (k_{obs}) were measured under single-turnover conditions as shown in Figures 2B and 5C. Using data from three independent series, the mean values were fitted to a one phase associate model for the calculation of k_{obs} (min^{-1}).
[a] KCCK = K249C C253K.

cleavage is inhibited in presence of free 8oxoG and physiological concentrations of Mg^{2+} (Morland et al., 2005), suggesting that hOgg1 will remain bound to an intact abasic site after base excision. This is in line with several studies showing stimulation of the Ogg1 DNA glycosylase activity by the major human AP endonuclease APE1 leading to bypass of the AP lyase step (Hill et al., 2001; Vidal et al., 2001) and an ~5- to 6-fold increase in the base hydrolysis reaction. Moreover, it has been demonstrated that the 5′-dRPase activity of Pol β is essential for the repair of 8oxoG in DNA by mammalian cell extracts (Allinson et al., 2001), hence processing of the abasic sites after removal of 8oxoG is thus initiated by AP endonuclease, followed by the 5′-dRPase activity of Pol β. This is consistent with our data supporting that removal of 8oxoG by hOgg1 occurs by base hydrolysis via the monofunctional branch of the BER pathway (Figure 1B) to give uncleaved AP sites as the major reaction product.

The present results demonstrate that hOgg1 possesses a monofunctional reaction modus for base removal, which operates independently of the β-elimination reaction. To compare the substrate affinity of the KCCK and WT hOgg1, the enzymes were incubated with duplex DNA containing 8oxoG or the AP site analog THF and analyzed by electrophoretic mobility shift assays (EMSA). The KCCK mutant bound abasic DNA with higher affinity than WT enzyme, whereas the WT enzyme appears to bind 8oxoG with higher affinity than the KCCK mutant (Figures 2C and 2D). Further, surface plasmon resonance (SPR) spectroscopy showed that the association rate (k_a) to AP sites was slightly higher for KCCK than for WT hOgg1, while the dissociation rate constant (k_d) is ten times higher for the WT enzyme (Figure 3 and Table 2). These data demonstrated that the KCCK mutant retained the capacity to bind abasic DNA despite the lack of AP lyase activity.

Asp268 Catalyzes 8oxoG Base Hydrolysis

To test if the conserved Asp268 is involved in the uncoupled monofunctional mechanism of hOgg1, a triple mutant K249C/C253K/D268N (KCCKDN) was designed. The triple mutant

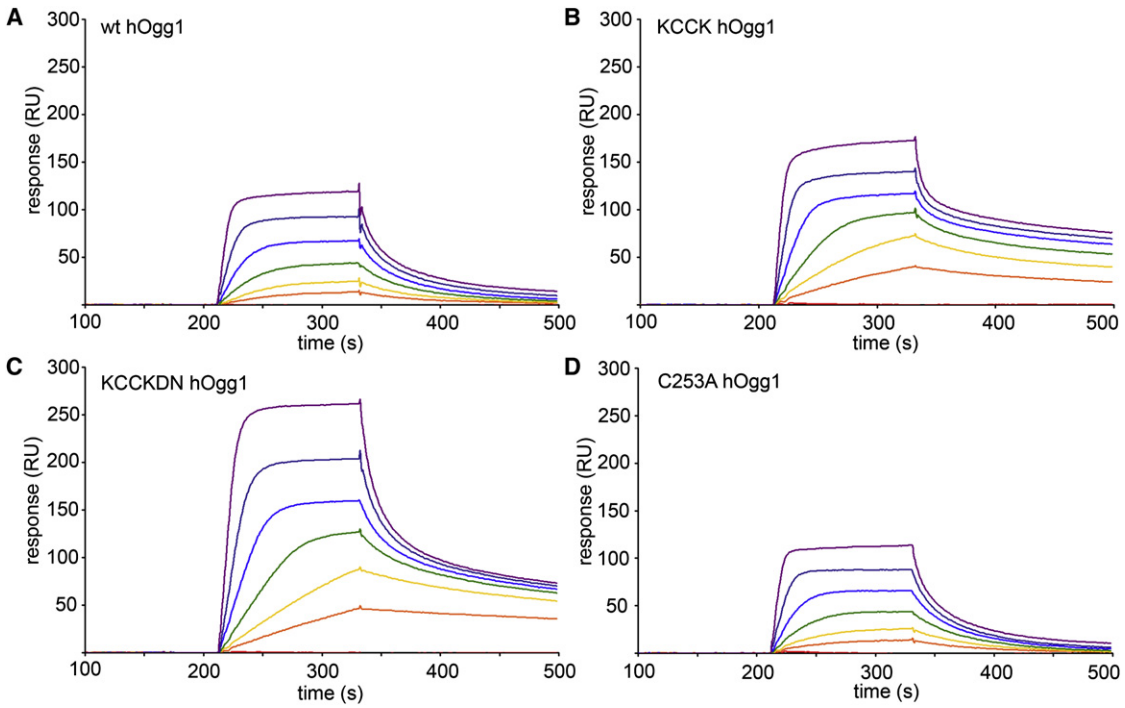

Figure 3. SPR Sensograms Displaying Binding and Dissociation of hOgg1 to Oligonucleotides Containing Abasic Sites Immobilized on Chips
(A) Wild-type hOgg1; (B) inverted dipole KCCK hOgg1 mutant; (C) KCCKDN hOgg1 triple mutant; (D) dipole-deficient C253A hOgg1 mutant. The colored lines represent a series of dilutions of the respective wild-type and mutant hOgg1 proteins: 16.0 nM (violet), 8.0 nM (indigo), 4.0 nM (blue), 2.0 nM (green), 1.0 nM (yellow), 0.5 nM (orange), and 0 nM (red).

Table 2. DNA Binding Kinetics of hOgg1 Wild-Type and Mutant Proteins Determined by Surface Plasmon Resonance Using DNA Substrate Containing the Abasic Site Analog THF

Protein	k_a ($M^{-1}s^{-1}$)	k_d (s^{-1})	k_d (M)
WT	5.6×10^6	0.019	3.3×10^{-9}
C253A	5.8×10^6	0.018	3.1×10^{-9}
KCCK[a]	6.6×10^6	0.0020	3.1×10^{-10}
KCCKDN[b]	1.1×10^7	0.0019	1.7×10^{-10}

Values are extracted from curve-fitting using a 1:1 Langmuir model.
[a] KCCK = K249C C253K.
[b] KCCKDN = K249C C253K D268N.

bound both 8oxoG and abasic DNA with comparable affinity as for WT hOgg1 as showed by EMSA (see Figure S1A available online). Neither wild-type nor any of the hOgg1 mutants bound to undamaged DNA (Figure S1B). SPR experiments showed that the association rate constant to abasic DNA was two times higher for the triple mutant than WT, while the dissociation rate constant was ten times lower for the triple mutant (Figure 3; Table 2). However, the triple mutant is completely devoid of both DNA glycosylase and AP lyase activity demonstrating that Asp268 is the catalytic residue in the monofunctional base hydrolysis reaction (Figure 2A, lanes 4 and 9).

Structure of KCCKDN Triple Mutant hOgg1

The crystal structure of the triple KCCKDN mutant of hOgg1 in complex with 8oxoG-containing DNA was determined to 1.55Å resolution (Figures 4A–4E and Table 3). At this resolution, the position and conformation of both the 8oxoG lesion and the mutated amino acid residues are unambiguous (Figures 4C and 4D). The structure reveals that the side-chain amino group of Lys253 is forming an "inverted" dipole with the partner Cys249 (2.6 Å distance), and is located approximately 4.7 Å from the anomeric C1' atom of the 8oxoG ribose (Figure 4E), to

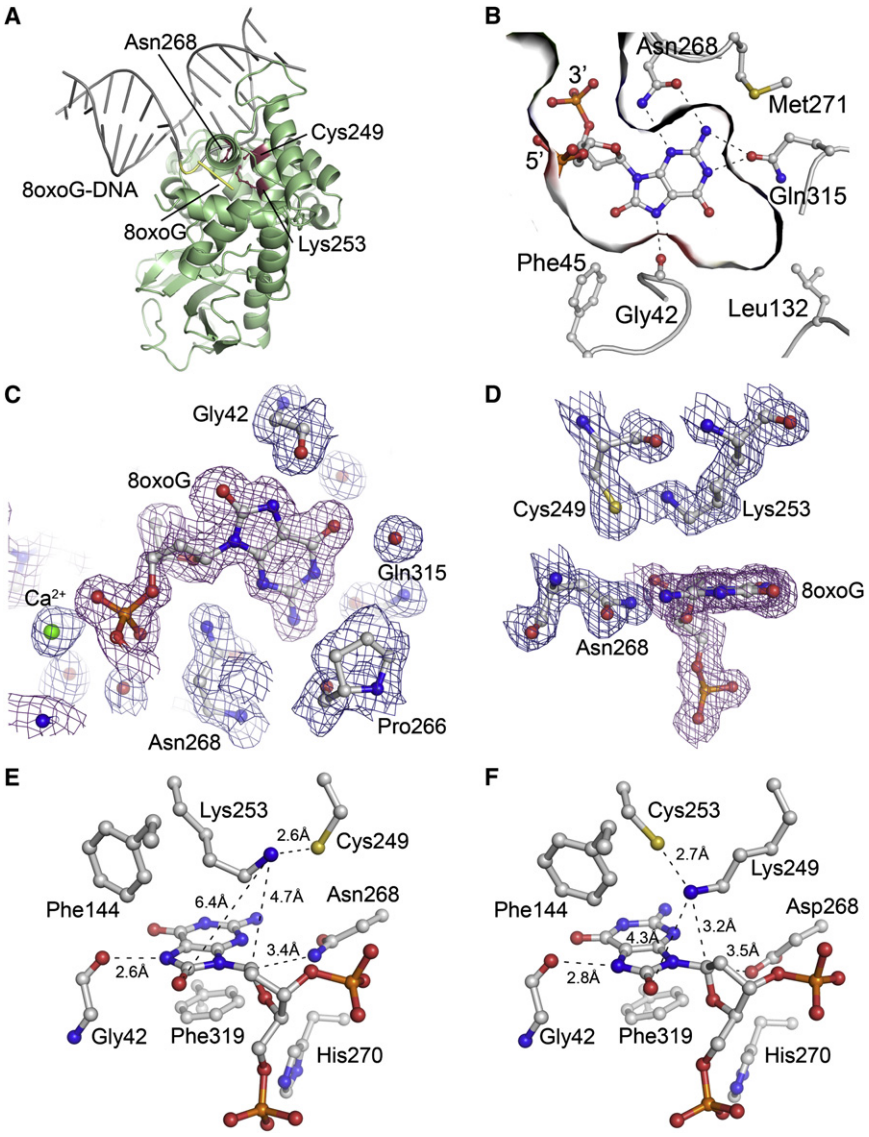

Figure 4. Structure of hOgg1 Triple Mutant in Complex with 8oxoG-Containing DNA

(A) Overall structure of the hOgg1 8oxoG-DNA complex. Mutated residues highlighted in red, 8oxoG base shown in yellow.

(B) Close-up view of the 8oxoG base in the active site of triple mutant KCCKDN hOgg1. Ball-and-stick display of 8oxoG and selected interacting residues forming the tight base-binding pocket (thin slab of the protein surface in the plane of the base). Hydrogen bond interactions with 8oxoG are indicated with dashed lines.

(C) Electron density map (composite omit map, contoured at 1σ) showing the position of the 8oxoG (pink density) relative to selected residues in the active site (blue density).

(D) Electron density map (composite omit map, contoured at 1σ) showing the conformation of the mutated Cys249 and Lys253 residues (blue density) and 8oxoG (pink density).

(E) Close-up view of selected interactions with Cys249, Lys253, and Asn268 in the active site pocket of the triple mutant.

(F) Close-up view of the corresponding interactions in the S292C/Q315F mutant of hOgg1 (Radom et al., 2007). Molecular superposition of the two structures is available in the supplemental material (Figure S2).

All panels were prepared by PyMOL (http://pymol.org).

Table 3. Summary of X-Ray Data Collection and Refinement Statistics for the Complex between the Triple Mutant KCCKDN hOgg1 and 8oxoG-Containing DNA

	KCCKDN hOgg1
Data collection	
Space group	$P6_522$
Unit-cell dimensions	
a (Å)	92.70
b (Å)	92.70
c (Å)	210.99
Resolution range (Å)	42–1.55
Last resolution shell (Å)	1.63–1.55
R_{sym} (%)	5.6 (58.3)
Average I / σI	14.5 (2.3)
Completeness (%)	99.5 (99.6)
Redundancy	5.8 (5.5)
Refinement	
Resolution (Å)	25–1.55
No. reflections	73,237
R_{work}/R_{free} (%)	22.9/26.5
No. atoms	
Protein	2518
Ligand/ion	578
Water	399
B-factors	
Protein	22.4
Ligand/ion	53.8
Water	35.2
Rmsd	
Bond lengths (Å)	0.025
Bond angles (°)	2.3
Ramachandran plot	
Residues in most favored regions (%)	95
Residues in additionally allowed regions (%)	4
Residues in disallowed regions (%)	1

Values in parentheses are for highest resolution shell.

which the covalent bond is formed in the Schiff base intermediate in the AP lyase reaction. The equivalent distance is only 3.2 Å in the structure of the S292C/Q315F double mutant of hOgg1 in complex with 8oxoG (Figure 4F), which is believed to represent a very late intermediate in the base extrusion process immediately prior to catalysis (Radom et al., 2007). The larger distance in the "dipole-inverted" mutant explains the loss of AP lyase activity. On the other hand, the mutated Asn268 has almost identical conformation and orientation as Asp268 in the very same S292C/Q315F mutant. Indeed, except for the two interchanged residues, the active site structure tolerates this side-chain swapping with limited perturbations (Figure S2). The Asn268 to C1' distance is 3.4 Å in the triple mutant, compared with 3.5 Å for the late-extrusion complex (Figures 4E and 4F). The present structure thus strongly supports a role for Asp268 as a key catalytic residue for the base hydrolysis reaction of hOgg1.

Lys249 Is Indispensable for 8oxoG Recognition

There is still no consensus in the literature on how Ogg1 and Fpg/MutM are able to distinguish between unmodified G and the oxidized 8oxoG, which only differ in the N7 and C8 positions (Figure 1A). The first structures of hOgg1 and Fpg in complex with DNA containing 8oxoG revealed no direct contact between the protein and the 8oxo group, but a hydrogen bond between the N7-hydrogen of 8oxoG and the protein backbone carbonyl of Gly42 (Figure 4B) (Bruner et al., 2000; Fromme and Verdine, 2002). These structures suggested that the N7 interaction serves as a sensor to discriminate 8oxoG and guanine. However, several biochemical studies point to a more elaborate mechanism for substrate recognition, as several substrates without the N7-hydrogen, like Me-faPyG and 7-methyl-8oxoG, are indeed processed by hOgg1 (Asagoshi et al., 2000; David et al., 2007; Hamm et al., 2007). Together, these data suggest that interaction with O8 rather than recognition of the N7-hydrogen atom is the key factor in the recognition mechanism for Ogg1 and Fpg. We find that the dipole-inverted double mutant of hOgg1 is still able to recognize 8oxoG and remove the oxidized lesion through a classical monofunctional mechanism using Asp268 only as the catalytic residue (Figure 2A, lanes 3 and 8). Mutation of Lys249 gives totally inactive mutants, despite having the active site residue Asp268 (Nash et al., 1997). This strongly suggests that the major role of Lys249 is to recognize the 8oxo group, either intrahelically, during base flipping, or in the final positioning of the lesion. Specifically, the trapping of the structure of WT Ogg1 bound to undamaged guanine flipped into an exo site (Banerjee et al., 2005) suggests that Lys249 plays an important part in the final positioning of the oxidized base in the active site since nonoxidized guanine can also be flipped out of the DNA helical stack. The recent structure of the Ogg1 S292C/Q315F mutant (Radom et al., 2007) demonstrates how geometrically demanding the transition state for base hydrolysis is. This hOgg1 mutant contains both active site residues Lys249 and Asp268, yet the flipped 8oxoG is not removed by the enzyme during crystallization. Evidently from the biochemical data, Lys253 in the inverted dipole mutant is still close enough to interact with the substrate and promote base flipping (Figures 4E and 4F) yet unable to catalyze an AP lyase/β-elimination (Figure 2A, lanes 2 and 3). For the KCCK mutant, we observed less than 20% Schiff base formation as compared with the WT hOgg1 (data not shown); however, the complete lack of any DNA incision product for this mutant (Figure 2A) demonstrates that the residual Schiff base complex is nonproductive.

From the present biochemical and structural analysis of our separation-of-function mutants of human Ogg1, we propose that the AP lyase activity of WT hOgg1 is probably a secondary effect of the need of having the ε-amino group of Lys249 in the active site for recognition of oxidized bases like 8oxoG and faPyG, which also places it simultaneously close to the anomeric C1′ in 8oxoG or the corresponding AP site. A comparable case has been described for the *E. coli* DNA glycosylase MutY, where two opportunistically positioned Lys residues (Lys120 and Lys142) are reported to form Schiff bases with abasic DNA (Guan et al., 1998; Manuel et al., 2004), while the major activity of MutY still seems to be monofunctional (Williams and David, 1998, 1999). These MutY protein-DNA Schiff base complexes are nonproductive complexes in the sense that no

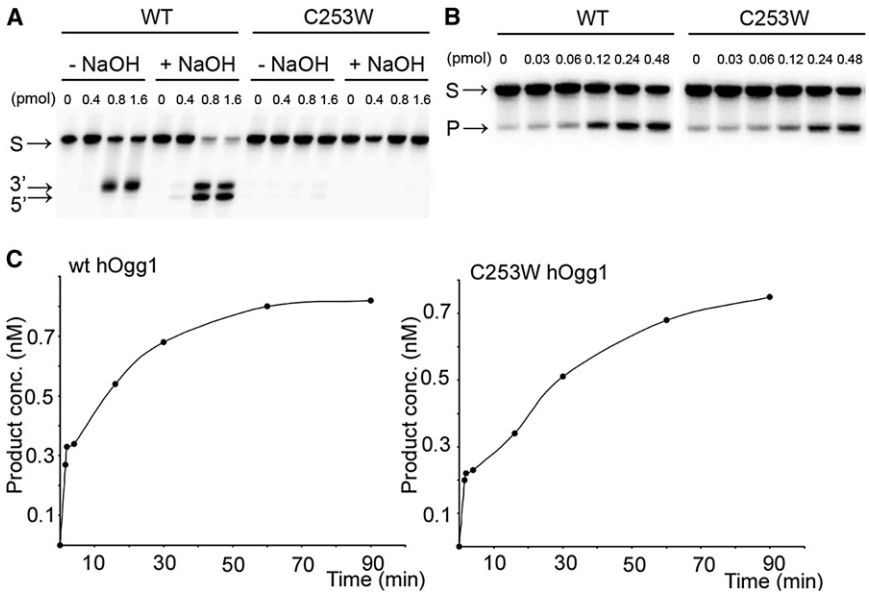

Figure 5. Biochemical and Kinetics Analysis of the AP Lyase Separation-of-Function C253W Mutant of hOgg1

(A) 8oxoG DNA cleavage assay of WT and C253W hOgg1 as a function of increasing amounts of protein. 0–1.6 pmol of protein was mixed with 10 fmol substrate DNA and incubated at 37°C for 30 min.

(B) AP lyase activity of WT and C253W hOgg1. 0–0.48 pmol of protein was mixed with 10 fmol substrate DNA and incubated at 37°C for 30 min.

(C) Single-turnover analysis of WT and C253W hOgg1 activity on abasic DNA. Curves show representative time course series. Using the mean values of three independent experiments, a fit to a one phase associate model was used for the calculation of the catalytic turnover rate k_{obs} (min^{-1}).

β- or δ-elimination process resolves these complexes and promote AP lyase strand cleavage (Zharkov et al., 2000a; Zharkov and Grollman, 1998). Instead, it is suggested that Lys142 in MutY is involved in final positioning of the dA:dG mismatch substrate (Zharkov et al., 2000a). Similar to hOgg1, the human endonuclease III (hNth1) shows uncoupling of base excision and phosphodiester incision with a 7-fold difference in activity in favor of base hydrolysis (Marenstein et al., 2001). Further, addition of human APE1 leads to abrogation of AP lyase activity and an increased turnover in base hydrolysis by hNth1 (Marenstein et al., 2003).

Notably, all bifunctional DNA glycosylases remove oxidative base lesions and contain active site lysine residues able to form Schiff bases. In view of the data presented here, it is tempting to suggest that these lysine residues are essential for recognition of oxidative base lesions and that their concurrent proximity to the anomeric C1' atoms permit these residues to participate in Schiff base-mediated β-elimination reactions in an opportunistic way, and in some instances also forming nonproductive Schiff base complexes.

Lys-Cys Dipole Is Not Imperative for 8oxoG Recognition

To pursue our initial observation that inversion of the $Lys249^{+}$-$Cys253^{-}$ dipole does not substantially affect processing of 8oxoG, as demonstrated by the 8oxoG excision activity by the KCCK mutant (Figure 2A), we also designed a "dipole-deficient" C253A mutant. This mutant, which lacks the negative partner of the dipole but otherwise contains all active site residues, showed both AP lyase activity (Figure 2A, lane 5) and base hydrolysis (Figure 2A, lane 10). The single-turnover rate for the C253A is similar to the 'inverted-dipole' KCCK mutant (Figure 2B and Table 1). Electrophoresis mobility shift assay demonstrated that the C253A mutant bound abasic DNA with similar affinity as the WT enzyme, but weaker for the 8oxoG substrate (Figure S1). Moreover, plasmon surface experiments showed that the association (k_a) and dissociation rate constant (k_d) to AP sites were similar for C253A and WT hOgg1 (Figure 3 and Table 2). It thus appears that the dipole is not essential for substrate recognition and catalysis. A structure of WT hOgg1 in complex with 8oxoG, representing a very late intermediate in the base-flipping trajectory (Lee et al., 2008), indeed reveals that the dipole is formed after final alignment of the substrate in the active site pocket, in agreement with our present interpretations.

While some nonphysiological product analogs of free 8oxoG such as 8-bromoguanine (8bromoG) and 8-aminoguanine (8aminoG) seems to enhance the AP lyase reaction (Fromme et al., 2003; Kuznetsov et al., 2005), the incision activity is inhibited by the released 8oxoG by the monofunctional hydrolysis of the canonical 8oxoG substrate (Morland et al., 2005). Based on our proposition that Lys249 is mainly involved in oxidative lesion recognition, a plausible explanation to these apparently contrasting observations can be put forward. In the case of 8oxoG, the positively charged ε-amino group of Lys249 may possibly be engaged and conformationally locked by strong hydrogen bonding with the liberated 8oxoG moiety, thus unable to charge a nucleophilic attack on C1′. The interaction with 8bromoG and 8aminoG will be much weaker, leaving Lys249 free to relocate and participate in AP lysis as suggested (Fromme et al., 2003).

hOgg1 AP Lyase-Only Separation-of-Function Mutant

Since we were able to design the monofunctional separation-of-function KCCK mutant of Ogg1, we also aimed to design the reverse separation-of-function mutant, a pure AP lyase hOgg1. We reasoned that by blocking the 8oxoG recognition pocket using a bulky amino acid side chain, it should be possible to design a hOgg1 mutant unable to flip 8oxoG nucleotides in DNA, but still able to recognize and cleave abasic DNA. By pursuing our observations that Cys253 is not critical for 8oxoG recognition (Figure 2A) and thus replacing the nonessential Cys253 in the dipole with Trp, we were able to design a pure AP lyase mutant of hOgg1. The C253W hOgg1 mutant was not cleaving 8oxoG-containing DNA (Figure 5A), but showed clear AP lyase activity on abasic DNA (Figure 5B). A time course analysis showed that wild-type hOgg1 processed abasic DNA five

times faster than the pure AP lyase mutant (Figure 5C and Table 1). The C253W mutant clearly demonstrates that the 8oxoG recognition pocket is not required for abasic site detection and flipping, nor does the Trp side chain prevent Lys249 from forming the Schiff base intermediate in the AP lyase reaction.

EXPERIMENTAL PROCEDURES

Plasmids, Constructs, and Site-Directed Mutagenesis

Full-length human Ogg1 cDNA was released from pUC18hOgg1 (Bjørås et al., 1997) by digestion with EcoRI and BamHI and subcloned into the EcoRI and BglII sites of pETDuet1 (Novagen) to give an N-terminal hexahistidine tag fused to hOgg1. Site-directed mutagenesis was performed according to the QuikChange mutagenesis protocol (Stratagene). The K249C and C253K mutations were simultaneously introduced by use of a single oligonucleotide and a complementary oligo, implementing two new codons to give the 'inverted dipole' mutant (KCCK hOgg1): 5′-ctgcctggagtgggcacc**tgc**gtggctgac**aag** atctgcctgatggcccta -3′. The triple mutant K249C/C253K/D268N mutant was designed by a subsequent round of mutagenesis using the oligonucleotide 5′-caggctgtgcccgtg**aat**gtccatatgtggc-3′ to replace Asp268 by Asn. The single mutant C253A was designed using the oligonucleotide 5′-ggcaccaaggtggct gac**gcc**atctgcctgatggccc-3′. The mutant constructs were verified by sequencing of the full-length hOgg1, and the respective expression plasmids were transformed into the *E. coli* BL21(DE3) RIL Codon Plus cells (Stratagene) for protein expression.

Protein Expression and Purification

Cells containing plasmids of wild-type, KCCK, KCCKDN, and C253A hOgg1 were grown in LB medium supplemented with sorbitol (0.5 M), betain (2.5 mM), and ampicillin (100 μg ml^{-1}). Protein expression was induced when the cell density reached an OD_{600} of ~0.75 by adding 1 mM IPTG. Induced cells were grown for 18 hr at 18°C, prior to harvesting by centrifugation. Cell pellets were resuspended in 300 mM NaCl, 50 mM Na_2HPO_4/NaH_2PO_4 (pH 8) and 10 mM 2-mercaptoethanol (2-ME) (buffer A). Crude extracts were prepared by sonication, and the extracts were applied to nickel NTA-agarose columns pre-equilibrated with buffer A. Unbound proteins were removed by extensive washing with buffer A supplemented with 50 mM imidazole. hOgg1 were eluted with 300 mM imidazole in buffer A. Fractions rich in hOgg1 were pooled and dialyzed against 50 mM NaCl, 10 mM MES (pH 6.0) and 10 mM 2-ME (buffer B), and applied to a Resource S column (GE Lifesciences) equilibrated with buffer B. The proteins were eluted with a salt gradient to 2 M NaCl in buffer B. Protein fractions pure in hOgg1 were identified by SDS-PAGE gel, pooled, and concentrated. Protein solutions for assays were supplemented with 20% glycerol prior to storage at −80°C. The protein solution for crystallization was further dialyzed against buffer B, concentrated to 20 mg ml^{-1} using a 10 kDa cut-off centrifugal filter (Amicon, Millipore) and stored at −20°C. Protein concentrations were determined by the Bio-Rad protein assay (Bio-Rad Laboratories, Inc.).

Preparation of DNA Substrates

The single-stranded DNA oligomers 5′- GGCGGCATGACCC[8oxoG]GAGGCC CATC-3′, 5′-ACCGAATTCTGACTTGCTA[THF]GACATCTTTGCCCACGTTGA-3′ and 5′-GCATGCCTGCACGG[U]CATGGCCAGATCCCCGGGTACCGAG-3′ (U = uracil) were 5′ end labeled with T4 polynucleotide kinase and [γ-^{32}P]ATP (NEN, Perkin Elmer). The labeled oligonucleotides were annealed with a complementary oligonucleotide to give the double-stranded substrates 8oxoG:C, THF:C and U:C, respectively. The G:C substrate had the same sequence as the THF substrate, with a normal G instead of the abasic site analog THF. The ^{32}P-labeled DNA substrates were purified on a 20% native polyacrylamide gel, and the radiolabeled bands were excised from the gel and eluted in H_2O and stored at 4°C. Prior to use, the uracil-substrate was treated with uracil DNA glcosylase (NEB) for 15 min at 37°C and heat inactivated at 55°C for 10 min to generate abasic DNA. All DNA oligos were purchased from Eurofins MWG Operon and purified by desalting.

Electrophoretic Mobility Shift Assay

DNA binding of the wild-type and various hOgg1 mutants was determined by EMSA. The end-labeled substrates 8oxoG:C and THF:C were incubated with enzyme as indicated at 4°C for 15 min in a total reaction volume of 10 μl of buffer containing 70 mM 3-(N-morpholino) propane sulphonic acid (pH 7.5), 1 mM EDTA, 5% glycerol, and 1 mM DTT. Undamaged and unlabeled competitor DNA (same oligonucleotide as for the G:C substrate) was added in 50-fold excess. Following incubation, samples were analyzed by 10% nondenaturing PAGE in 0.5× TBE at 4°C and visualized by phosphorimaging. Three parallel experiments were performed and representative gels are shown (Figures 2C and 2D). Neither the wild-type nor hOgg1 mutants showed any activity for 8oxoG under the conditions used in the EMSA assay (data not shown).

Surface Plasmon Resonance Spectroscopy

Binding of hOgg1 wild-type and mutant proteins to DNA containing the abasic site analog THF was monitored using SPR spectroscopy. Binding experiments were carried out on a BiaCore 3000 SPR biosensor, using DNA immobilized on SA chips. In brief, sensor chips coated with streptavidin were treated with 1 M NaCl in 40 mM NaOH to prepare the streptavidin surface for binding of biotin-labeled DNA. The single-stranded DNA oligomer 5′-gctcatgcgcag[THF] cagccgtactcg-3′ was annealed with a 5′-biotinyl-labeled, complementary oligonucleotide to give the double-stranded THF:C substrate (oligos from Eurofins MWG Operon). The biotinylated DNA-duplex was diluted to 5 nM in HBS-EP buffer (150 nM NaCl, 3 mM EDTA, 0.005% P-20, 10 mM HEPES [pH 7.4]), and injected to the sensor chip surface at a flow rate of 20 μl/min. Five hundred response units (RU) were immobilized onto the chip, followed by 1 min washing with HBS-EP buffer. The sensograms for DNA-hOgg1 interactions were recorded for a series of hOgg1 concentrations (0–16.0 nM protein) in real time and were analyzed after subtracting the sensogram from the blank channel (Figure 3). The BIA evaluation software version 4.1 was used to calculate the binding kinetics. The simple 1:1 Langmuir model was used to fit the data. The degree of randomness of residual plots and the reduced chi-square values were used to determine the accuracy of the fits. In the Langmuir model k_a and k_d represent the association and dissociation rate constants, respectively. The dissociation constant, K_D, is calculated by dividing k_d by k_a.

DNA Glycosylase/AP Lyase Assay

DNA glycosylase and/or AP lyase activity of the wild-type and various hOgg1 mutants were determined by incubation of 10 fmol 8oxoG:C or abasic site containing DNA with enzymes as indicated at 37°C for 30 min. The assays were performed in a total volume of 10 μl of a reaction buffer containing 70 mM 3-(N-morpholino) propane sulphonic acid (pH 7.5), 1 mM EDTA, 5% glycerol and 1 mM DTT. To detect any uncleaved abasic DNA product formed by a monofunctional reaction, one part of the product mixture was heated to 70°C for 15 min in 100 mM NaOH and neutralized with 100 mM HCl to cleave the abasic DNA. Formamide DNA loading buffer (90% formamide with 0.05% bromphenol blue and 0.05% xylene cyanol) was added and the samples heated to 90°C for 3 min prior to loading on the gel. In samples not treated with NaOH, formamide DNA loading buffer was added directly to stop the reactions. The samples were heated to 90°C for 3 min prior to loading on the gel. All samples were analyzed by 20% denaturing PAGE in 1× taurine at 20°C and visualized by phosphorimaging. Three parallel experiments were performed and representative gels are shown (Figures 2A, 5B, and 5C).

Single-Turnover Kinetic Analysis

The kinetic constant k_{obs} for removal of 8oxoG or abasic site incision under single-turnover conditions were determined by incubating 10 nM hOgg1 wild-type and mutant proteins with 1 nM of 8oxoG:C or abasic DNA substrate at 37°C. To determine the level of base removal, reactions were stopped at selected time points by adding 100 mM NaOH, heated to 70°C for 15 min and neutralized with 100 mM HCl. Finally the samples were analyzed by 20% PAGE and phosphorimaging as described above to calculate the amount of product formed. Using data from three independent series, the mean values were fitted to a one phase associate model for the calculation of the catalytic turnover rates k_{obs} (min^{-1}) using the Origin 8.1 software (OriginLab Corp., Northampton, MA).

Crystallization, Data Collection, Structure Solution, and Model Refinement

Synthetic oligonucleotides 5′-GGTAGACCTGGACGC-3′ and 5′-GCGTCCA-8oxoG-GTCTACC-3′ (Eurofins MWG Operon; salt-free grade) annealed to

yield a blunt-end 8oxoG:C substrate. The duplex DNA product was mixed in a 1.5:1 ratio (excess DNA) with the purified full-length triple mutant KCCKDN hOgg1 still fused to the hexahistidine tag (20 mg ml^{-1}) in 20 mM Tris (pH 7.4), 100 mM NaCl, 1 mM EDTA, and 5 mM DTT. The reaction mixture was incubated for 30 min on ice. Large, rod-shaped crystals were formed at room temperature in hanging drops made by mixing 1 μl of protein-DNA solution with 1 μl of reservoir solution consisting of 100 mM sodium cacodylate (pH 6.5), 100 mM $CaCl_2$, and 18%–24% Peg8000. Crystals were briefly soaked in reservoir solution with additional Peg400 to a final concentration of 15% prior to flash freezing in liquid nitrogen. A high-resolution data set was collected at the ID14-2 beamline, ESRF/Grenoble. Diffraction images were processed with Mosflm (Leslie, 1992) and scaled with Scala/CCP4 (CCP4, 1994). The crystal belong to the $P6_522$ space group with cell parameters $a = b = 92.70$ Å and $c = 210.99$ Å. The structure was solved by molecular replacement using MolRep/CCP4 (Collaborative Computational Project Number 4, 1994) with the structure of the N149C/K249Q double mutant of hOgg1 in complex with 8oxoG-containing DNA (Banerjee et al., 2005) as a search model (PDB id 1yqr). Only coordinates for the protein part were used, and residues 249 and 253 were replaced by alanines. A clear solution was identified, and side chains were checked and adjusted to the correct conformation and type wherever needed, according to the F_o-F_c and $2F_o$-F_c Fourier maps. The initial protein model was refined in Refmac5/CCP4. The unambiguous density in the difference map for the central part of the DNA with 8oxoG flipped into the active site pocket allowed for gradual building and refinement of 29 of the total 30 nucleotides in the cocrystallized DNA. Finally, solvent water molecules were added in several consecutive rounds of automated water-picking in Coot, interspersed with refinement in Refmac5. Two of the water molecules were replaced by Ca^{2+} ions, based on the coordination geometry and knowledge from previous structures. Residue His282 has been modeled with two alternate conformations, and residues in the flexible loop 81-83 have been included, but the occupancy factor was set to zero during refinement as the electron density was very weak in this region. The final model, at 1.55 Å resolution, contain residues 10–325 of hOgg1, 29 nucleotides, two Ca^{2+} ions and 399 solvent water molecules. Crystal data and refinement parameters are summarized in Table 3.

ACCESSION NUMBERS

Coordinates and structure factors have been deposited in the Protein Data Bank under the accession code 2xhi.

SUPPLEMENTAL INFORMATION

Supplemental Information includes two figures and can be found with this article online at doi:10.1016/j.str.2010.09.023.

ACKNOWLEDGMENTS

The authors acknowledge the technical support at the ID14-2 beamline at ESRF, Grenoble, used to collect X-ray diffraction data. The authors declare that they have no conflict of interest. This work was supported by Norwegian Research Council (FUGE-CAMST) and the Norwegian Cancer Society.

Received: April 26, 2010
Revised: August 31, 2010
Accepted: September 30, 2010
Published: January 11, 2011

REFERENCES

Aburatani, H., Hippo, Y., Ishida, T., Takashima, R., Matsuba, C., Kodama, T., Takao, M., Yasui, A., Yamamoto, K., and Asano, M. (1997). Cloning and characterization of mammalian 8-hydroxyguanine-specific DNA glycosylase/apurinic, apyrimidinic lyase, a functional mutM homologue. Cancer Res. *57*, 2151–2156.

Allinson, S.L., Dianova, I.I., and Dianov, G.L. (2001). DNA polymerase beta is the major dRP lyase involved in repair of oxidative base lesions in DNA by mammalian cell extracts. EMBO J. *20*, 6919–6926.

Ames, B.N., Shigenaga, M.K., and Hagen, T.M. (1993). Oxidants, antioxidants, and the degenerative diseases of aging. Proc. Natl. Acad. Sci. USA *90*, 7915–7922.

Asagoshi, K., Yamada, T., Terato, H., Ohyama, Y., Monden, Y., Arai, T., Nishimura, S., Aburatani, H., Lindahl, T., and Ide, H. (2000). Distinct repair activities of human 7,8-dihydro-8-oxoguanine DNA glycosylase and formamidopyrimidine DNA glycosylase for formamidopyrimidine and 7,8-dihydro-8-oxoguanine. J. Biol. Chem. *275*, 4956–4964.

Asahara, H., Wistort, P.M., Bank, J.F., Bakerian, R.H., and Cunningham, R.P. (1989). Purification and characterization of Escherichia coli endonuclease III from the cloned nth gene. Biochemistry *28*, 4444–4449.

Aspinwall, R., Rothwell, D.G., Roldan-Arjona, T., Anselmino, C., Ward, C.J., Cheadle, J.P., Sampson, J.R., Lindahl, T., Harris, P.C., and Hickson, I.D. (1997). Cloning and characterization of a functional human homolog of Escherichia coli endonuclease III. Proc. Natl. Acad. Sci. USA *94*, 109–114.

Bailly, V., Verly, W.G., O'Connor, T., and Laval, J. (1989). Mechanism of DNA strand nicking at apurinic/apyrimidinic sites by Escherichia coli [formamidopyrimidine]DNA glycosylase. Biochem. J. *262*, 581–589.

Banerjee, A., Yang, W., Karplus, M., and Verdine, G.L. (2005). Structure of a repair enzyme interrogating undamaged DNA elucidates recognition of damaged DNA. Nature *434*, 612–618.

Barrett, T.E., Savva, R., Panayotou, G., Barlow, T., Brown, T., Jiricny, J., and Pearl, L.H. (1998). Crystal structure of a G:T/U mismatch-specific DNA glycosylase: mismatch recognition by complementary-strand interactions. Cell *92*, 117–129.

Bjørås, M., Luna, L., Johnsen, B., Hoff, E., Haug, T., Rognes, T., and Seeberg, E. (1997). Opposite base-dependent reactions of a human base excision repair enzyme on DNA containing 7,8-dihydro-8-oxoguanine and abasic sites. EMBO J. *16*, 6314–6322.

Bjørås, M., Seeberg, E., Luna, L., Pearl, L.H., and Barrett, T.E. (2002). Reciprocal "flipping" underlies substrate recognition and catalytic activation by the human 8-oxo-guanine DNA glycosylase. J. Mol. Biol. *317*, 171–177.

Boiteux, S., O'Connor, T.R., Lederer, F., Gouyette, A., and Laval, J. (1990). Homogeneous Escherichia coli FPG protein. A DNA glycosylase which excises imidazole ring-opened purines and nicks DNA at apurinic/apyrimidinic sites. J. Biol. Chem. *265*, 3916–3922.

Bruner, S.D., Norman, D.P., and Verdine, G.L. (2000). Structural basis for recognition and repair of the endogenous mutagen 8-oxoguanine in DNA. Nature *403*, 859–866.

CCP4 (Collaborative Computational Project Number 4). (1994). The CCP4 suite: programs for protein crystallography. Acta Crystallogr. D. Biol. Crystallogr. *50*, 760–763.

Dalhus, B., Helle, I.H., Backe, P.H., Alseth, I., Rognes, T., Bjoras, M., and Laerdahl, J.K. (2007). Structural insight into repair of alkylated DNA by a new superfamily of DNA glycosylases comprising HEAT-like repeats. Nucleic Acids Res. *35*, 2451–2459.

Dalhus, B., Laerdahl, J.K., Backe, P.H., and Bjoras, M. (2009). DNA base repair–recognition and initiation of catalysis. FEMS Microbiol. Rev. *33*, 1044–1078.

David, S.S., O'Shea, V.L., and Kundu, S. (2007). Base-excision repair of oxidative DNA damage. Nature *447*, 941–950.

Dodson, M.L., Michaels, M.L., and Lloyd, R.S. (1994). Unified catalytic mechanism for DNA glycosylases. J. Biol. Chem. *269*, 32709–32712.

Fromme, J.C., and Verdine, G.L. (2002). Structural insights into lesion recognition and repair by the bacterial 8-oxoguanine DNA glycosylase MutM. Nat. Struct. Biol. *9*, 544–552.

Fromme, J.C., and Verdine, G.L. (2003). Structure of a trapped endonuclease III-DNA covalent intermediate. EMBO J. *22*, 3461–3471.

Fromme, J.C., Bruner, S.D., Yang, W., Karplus, M., and Verdine, G.L. (2003). Product-assisted catalysis in base-excision DNA repair. Nat. Struct. Biol. *10*, 204–211.

Guan, Y., Manuel, R.C., Arvai, A.S., Parikh, S.S., Mol, C.D., Miller, J.H., Lloyd, S., and Tainer, J.A. (1998). MutY catalytic core, mutant and bound adenine

structures define specificity for DNA repair enzyme superfamily. Nat. Struct. Biol. *5*, 1058–1064.

Hamm, M.L., Gill, T.J., Nicolson, S.C., and Summers, M.R. (2007). Substrate specificity of Fpg (MutM) and hOGG1, two repair glycosylases. J. Am. Chem. Soc. *129*, 7724–7725.

Hazra, T.K., Izumi, T., Boldogh, I., Imhoff, B., Kow, Y.W., Jaruga, P., Dizdaroglu, M., and Mitra, S. (2002a). Identification and characterization of a human DNA glycosylase for repair of modified bases in oxidatively damaged DNA. Proc. Natl. Acad. Sci. USA *99*, 3523–3528.

Hazra, T.K., Kow, Y.W., Hatahet, Z., Imhoff, B., Boldogh, I., Mokkapati, S.K., Mitra, S., and Izumi, T. (2002b). Identification and characterization of a novel human DNA glycosylase for repair of cytosine-derived lesions. J. Biol. Chem. *277*, 30417–30420.

Hegde, M.L., Hazra, T.K., and Mitra, S. (2008). Early steps in the DNA base excision/single-strand interruption repair pathway in mammalian cells. Cell Res. *18*, 27–47.

Hill, J.W., Hazra, T.K., Izumi, T., and Mitra, S. (2001). Stimulation of human 8-oxoguanine-DNA glycosylase by AP-endonuclease: potential coordination of the initial steps in base excision repair. Nucleic Acids Res. *29*, 430–438.

Kasai, H., Crain, P.F., Kuchino, Y., Nishimura, S., Ootsuyama, A., and Tanooka, H. (1986). Formation of 8-hydroxyguanine moiety in cellular DNA by agents producing oxygen radicals and evidence for its repair. Carcinogenesis *7*, 1849–1851.

Kow, Y.W., and Wallace, S.S. (1987). Mechanism of action of Escherichia coli endonuclease III. Biochemistry *26*, 8200–8206.

Krokan, H.E., Standal, R., and Slupphaug, G. (1997). DNA glycosylases in the base excision repair of DNA. Biochem. J. *325*, 1–16.

Kuznetsov, N.A., Koval, V.V., Zharkov, D.O., Nevinsky, G.A., Douglas, K.T., and Fedorova, O.S. (2005). Kinetics of substrate recognition and cleavage by human 8-oxoguanine-DNA glycosylase. Nucleic Acids Res. *33*, 3919–3931.

Labahn, J., Scharer, O.D., Long, A., Ezaz-Nikpay, K., Verdine, G.L., and Ellenberger, T.E. (1996). Structural basis for the excision repair of alkylation-damaged DNA. Cell *86*, 321–329.

Lau, A.Y., Wyatt, M.D., Glassner, B.J., Samson, L.D., and Ellenberger, T. (2000). Molecular basis for discriminating between normal and damaged bases by the human alkyladenine glycosylase, AAG. Proc. Natl. Acad. Sci. USA *97*, 13573–13578.

Lavrukhin, O.V., and Lloyd, R.S. (2000). Involvement of phylogenetically conserved acidic amino acid residues in catalysis by an oxidative DNA damage enzyme formamidopyrimidine glycosylase. Biochemistry *39*, 15266–15271.

Lee, S., Radom, C.T., and Verdine, G.L. (2008). Trapping and structural elucidation of a very advanced intermediate in the lesion-extrusion pathway of hOGG1. J. Am. Chem. Soc. *130*, 7784–7785.

Leslie, A.G.W. 1992. Recent changes to the MOSFLM package for processing film and image plate data. Joint CCP4 + ESF-EAMCB Newsletter on Protein Crystallography 26.

Lindahl, T., and Wood, R.D. (1999). Quality control by DNA repair. Science *286*, 1897–1905.

Lu, R., Nash, H.M., and Verdine, G.L. (1997). A mammalian DNA repair enzyme that excises oxidatively damaged guanines maps to a locus frequently lost in lung cancer. Curr. Biol. *7*, 397–407.

Maiti, A., Morgan, M.T., Pozharski, E., and Drohat, A.C. (2008). Crystal structure of human thymine DNA glycosylase bound to DNA elucidates sequence-specific mismatch recognition. Proc. Natl. Acad. Sci. USA *105*, 8890–8895.

Manuel, R.C., Hitomi, K., Arvai, A.S., House, P.G., Kurtz, A.J., Dodson, M.L., McCullough, A.K., Tainer, J.A., and Lloyd, R.S. (2004). Reaction intermediates in the catalytic mechanism of Escherichia coli MutY DNA glycosylase. J. Biol. Chem. *279*, 46930–46939.

Marenstein, D.R., Ocampo, M.T., Chan, M.K., Altamirano, A., Basu, A.K., Boorstein, R.J., Cunningham, R.P., and Teebor, G.W. (2001). Stimulation of human endonuclease III by Y box-binding protein 1 (DNA-binding protein B). Interaction between a base excision repair enzyme and a transcription factor. J. Biol. Chem. *276*, 21242–21249.

Marenstein, D.R., Chan, M.K., Altamirano, A., Basu, A.K., Boorstein, R.J., Cunningham, R.P., and Teebor, G.W. (2003). Substrate specificity of human endonuclease III (hNTH1). Effect of human APE1 on hNTH1 activity. J. Biol. Chem. *278*, 9005–9012.

McCann, J.A., and Berti, P.J. (2008). Transition-state analysis of the DNA repair enzyme MutY. J. Am. Chem. Soc. *130*, 5789–5797.

Melamede, R.J., Hatahet, Z., Kow, Y.W., Ide, H., and Wallace, S.S. (1994). Isolation and characterization of endonuclease VIII from Escherichia coli. Biochemistry *33*, 1255–1264.

Mol, C.D., Arvai, A.S., Slupphaug, G., Kavli, B., Alseth, I., Krokan, H.E., and Tainer, J.A. (1995). Crystal structure and mutational analysis of human uracil-DNA glycosylase: structural basis for specificity and catalysis. Cell *80*, 869–878.

Morland, I., Luna, L., Gustad, E., Seeberg, E., and Bjoras, M. (2005). Product inhibition and magnesium modulate the dual reaction mode of hOgg1. DNA Repair (Amst.) *4*, 381–387.

Nash, H.M., Lu, R., Lane, W.S., and Verdine, G.L. (1997). The critical active-site amine of the human 8-oxoguanine DNA glycosylase, hOgg1: direct identification, ablation and chemical reconstitution. Chem. Biol. *4*, 693–702.

Norman, D.P., Bruner, S.D., and Verdine, G.L. (2001). Coupling of substrate recognition and catalysis by a human base-excision DNA repair protein. J. Am. Chem. Soc. *123*, 359–360.

Norman, D.P., Chung, S.J., and Verdine, G.L. (2003). Structural and biochemical exploration of a critical amino acid in human 8-oxoguanine glycosylase. Biochemistry *42*, 1564–1572.

Radicella, J.P., Dherin, C., Desmaze, C., Fox, M.S., and Boiteux, S. (1997). Cloning and characterization of hOGG1, a human homolog of the OGG1 gene of Saccharomyces cerevisiae. Proc. Natl. Acad. Sci. USA *94*, 8010–8015.

Radom, C.T., Banerjee, A., and Verdine, G.L. (2007). Structural characterization of human 8-oxoguanine DNA glycosylase variants bearing active site mutations. J. Biol. Chem. *282*, 9182–9194.

Roldan-Arjona, T., Wei, Y.F., Carter, K.C., Klungland, A., Anselmino, C., Wang, R.P., Augustus, M., and Lindahl, T. (1997). Molecular cloning and functional expression of a human cDNA encoding the antimutator enzyme 8-hydroxyguanine-DNA glycosylase. Proc. Natl. Acad. Sci. USA *94*, 8016–8020.

Rosenquist, T.A., Zharkov, D.O., and Grollman, A.P. (1997). Cloning and characterization of a mammalian 8-oxoguanine DNA glycosylase. Proc. Natl. Acad. Sci. USA *94*, 7429–7434.

Seeberg, E., Eide, L., and Bjoras, M. (1995). The base excision repair pathway. Trends Biochem. Sci. *20*, 391–397.

Vidal, A.E., Hickson, I.D., Boiteux, S., and Radicella, J.P. (2001). Mechanism of stimulation of the DNA glycosylase activity of hOGG1 by the major human AP endonuclease: bypass of the AP lyase activity step. Nucleic Acids Res. *29*, 1285–1292.

Werner, R.M., and Stivers, J.T. (2000). Kinetic isotope effect studies of the reaction catalyzed by uracil DNA glycosylase: evidence for an oxocarbenium ion-uracil anion intermediate. Biochemistry *39*, 14054–14064.

Wibley, J.E., Waters, T.R., Haushalter, K., Verdine, G.L., and Pearl, L.H. (2003). Structure and specificity of the vertebrate anti-mutator uracil-DNA glycosylase SMUG1. Mol. Cell *11*, 1647–1659.

Williams, S.D., and David, S.S. (1998). Evidence that MutY is a monofunctional glycosylase capable of forming a covalent Schiff base intermediate with substrate DNA. Nucleic Acids Res. *26*, 5123–5133.

Williams, S.D., and David, S.S. (1999). Formation of a Schiff base intermediate is not required for the adenine glycosylase activity of Escherichia coli MutY. Biochemistry *38*, 15417–15424.

Wood, R.D., Mitchell, M., Sgouros, J., and Lindahl, T. (2001). Human DNA repair genes. Science *291*, 1284–1289.

Zhang, X., Rosenstein, B.S., Wang, Y., Lebwohl, M., Mitchell, D.M., and Wei, H. (1997). Induction of 8-oxo-7,8-dihydro-2′-deoxyguanosine by ultraviolet radiation in calf thymus DNA and HeLa cells. Photochem. Photobiol. *65*, 119–124.

Zharkov, D.O., and Grollman, A.P. (1998). MutY DNA glycosylase: base release and intermediate complex formation. Biochemistry *37*, 12384–12394.

Zharkov, D.O., Gilboa, R., Yagil, I., Kycia, J.H., Gerchman, S.E., Shoham, G., and Grollman, A.P. (2000a). Role for lysine 142 in the excision of adenine from A:G mispairs by MutY DNA glycosylase of Escherichia coli. Biochemistry *39*, 14768–14778.

Zharkov, D.O., Rosenquist, T.A., Gerchman, S.E., and Grollman, A.P. (2000b). Substrate specificity and reaction mechanism of murine 8-oxoguanine-DNA glycosylase. J. Biol. Chem. *275*, 28607–28617.

Zharkov, D.O., Golan, G., Gilboa, R., Fernandes, A.S., Gerchman, S.E., Kycia, J.H., Rieger, R.A., Grollman, A.P., and Shoham, G. (2002). Structural analysis of an Escherichia coli endonuclease VIII covalent reaction intermediate. EMBO J. *21*, 789–800.

